Comprehensive power flow modelling of hierarchically controlled AC/DC hybrid islanded microgrids

Agundis Tinajero, Gibran David; Nasir, Mashood; Vasquez, Juan C.; Guerrero, Josep M.

Published in:
International Journal of Electrical Power and Energy Systems

DOI (link to publication from Publisher):
10.1016/j.ijepes.2020.106629

Publication date:
2021

Document Version
Early version, also known as pre-print

Comprehensive Power Flow Modelling of Hierarchically Controlled AC/DC Hybrid Islanded Microgrids

Gibran David Agundis Tinajero, Mashood Nasir, Juan C. Vasquez, and Josep M. Guerrero

Abstract

This paper presents the power flow modelling for AC/DC hybrid islanded microgrids including droop-controlled distributed generation units, secondary frequency and voltage restoration control for the AC side of the microgrid, and secondary voltage restoration control for the DC side of the microgrid. The interlink converter between the AC and DC microgrids includes a frequency-voltage droop control, and considers the effect of the secondary control for the AC microgrid side. Two case studies are presented for the power flow model evaluation, in the first case a microgrid with linear loads and equal droop characteristic for the distributed generation units are used; in the second case, voltage dependent loads for both AC and DC microgrids are included, and different droop characteristic are chosen for each distributed generation unit. Comparisons between the power flow solutions through the proposed modelling and the professional simulator MATLAB/Simulink are presented. Additionally, the computational speed and convergence rate of the power flow method are shown. The obtained results corroborate the reliability and effectiveness of the proposed power flow modeling to represent the controlled AC/DC hybrid microgrid including hierarchical controllers.

Index Terms

AC/DC hybrid microgrid, hierarchical control, power flow, Newton-Raphson method.

I. Introduction

WITH the extended penetration of AC and DC systems into the main power system, such as, renewable energy power plants, energy storage, and loads, there has been increasing research efforts for the development of AC/DC hybrid microgrids (MG), this is because the advantages of both AC and DC MGs can be combined, and a more efficient operation can be achieved [1]–[4]; however, since the microgrid concept brought a change of paradigm in traditional power systems [5], [6], different

Gibran David Agundis Tinajero, Mashood Nasir, Juan C. Vasquez, and Josep M. Guerrero are with the Aalborg university, 9220 Aalborg, Denmark

mathematical models and analysis techniques, for both transient and steady state, had to be evaluated and improved to cope with the especial operating characteristics of the AC and DC MGs [7], this is the case for the power flow method.

The power flow has been one of the most common and frequently performed mathematical techniques used in practical power systems; it plays an important role in analysis, planning and designing the future expansion of power systems as well as for economic scheduling, monitoring, and control of existing systems, among others [8]–[10]. In conventional power systems, the power flow studies are well-established with standard mathematical models and solving methodologies [9]. In those formulations, every bus falls into one type, for AC systems: voltage controlled bus (PV), load bus (PQ), and slack bus; for DC systems: PV bus, and load bus for only active power (PL), and in general, Gauss-Seidel and Newton-Raphson methods are used for solving the power flow problem. Nonetheless, it has been shown in the literature that in the MG case, due to the distributed generation (DG) units, some buses do not fall in any of the previous categories, this is mainly because the active and reactive power injected by the DG units is not known a priory and depend on the employed control scheme [11], [12]. In this way, for MGs there has been a need of power-flow-like mathematical models which can reproduce the controlled DG units steady-state behavior for different control schemes, with solutions as reliable as the ones obtained with the complete controlled MG, but with the advantages of the conventional power flow method.

In the literature, the development and evaluation of new power flow formulations for AC/DC hybrid microgrids has been carried out [1], [2], [13]–[15]. A Newton-Raphson-based power flow problem formulation is presented in [1], the authors include in the power flow buses the primary droop control for the AC and DC DG units, and a frequency-voltage droop control for the interlink converter. In [2], a power flow formulation for MGs with multiple AC/DC connections is presented, the AC and DC DG buses formulation includes the primary droop control, and for the interlink converter the frequency of the AC system is matched with the voltage of the DC system through a normalization, finally, the system is solved using GAMS. In [13], a hybrid AC/DC power flow is presented considering primary droop controls and virtual impedances for the DG units. A sequential power flow for droop controlled AC/DC hybrid microgrids is presented in [14]. In this formulation, the AC system is solved first using the Newton-Raphson formulation, then the interlink converter is updated and the DC system is solved; the iterations between the AC and the DC system continues until the convergence is attained. In [15], the authors present the formulation of the power flow problem including the primary droop control for both AC and DC MGs, furthermore, three voltage-frequency droop control schemes for the interlink converter are shown; the power flow equations for each component is presented, and the solution of the power flow problem is made using a Newton trust-region method.

Note that in the previous works only the primary droop controls were considered for the power flow problem formulation; however, in order to ensure an optimal, reliable, and secure operation of the microgrid, the inclusion of higher control levels have to be done in practical systems, i.e., hierarchical control schemes [16]. In this sense, and in regards to the power flow, it has been shown in a controlled AC microgrid that the steady-state solution obtained using only the primary droop controlled power flow approach differs from the solution obtained using the hierarchical power flow approach [17], being the correct solution the one which included the complete hierarchical control models. Note that hierarchical control schemes include primary, secondary and tertiary control levels, which have multiple operational time scales [18]; the primary and secondary controls have a close operational time scale, therefore, they affect the steady-state solution in a coupled way, however, the tertiary control level typically operates in the order of minutes [19], in consequence, its output can be considered as constant for the power flow modeling. In regards of the aforementioned, for an AC/DC hybrid microgrid, the inclusion of both primary and secondary controls in the DG units modelling is required for reliable steady-state analyses.

To cope with this gap, this paper presents the power flow modelling for AC/DC hybrid islanded microgrids including primary droop control for both AC and DC DG units, secondary frequency and voltage restoration control for the AC DG units, and secondary voltage restoration for the DC DG units. Additionally, a frequency-voltage droop control is included for the interlink converter, considering as well the effect of the secondary control for the AC side. Note that the interlink converter is a key component in AC/DC microgrids since it allows the power management between the AC and DC side in a controlled and stable way. The obtained power flow problem formulation is solved with the well-known Newton-Raphson method, having quadratic convergence regardless of the AC/DC MG topology. It is worth mentioning that the control schemes for AC subgrid, DC subgrid and interlinking converters used in this work are chosen owing to their wide use in the literature. There exist many other advanced AC/DC hybrid microgrids control schemes with improvements or modifications in the basic control scheme [4], [18], [20], [21]. Note that, each different control scheme will lead to a different power flow modeling formulation, therefore, considering different control approaches may lead to further research work. It should be highlighted that the conventional AC power flow algorithms are not directly valid for DC systems, due to the absence of frequency, and reactive power compoenents in DC systems. Therefore, these methods needs to be modified accordingly. The power-flow problem becomes even more challenging when both AC, and DC systems are present simultaneously, and can interact with each other. In such a scenario, modelling of interlinking converter, responsible for interaction between AC and DC system, needs to be included as well, for accurate power flow formulation. Therefore, the main contribution of this research is the joint power flow formulation of hierarchically controlled AC/DC microgrids together with the Interlink Converter; this joint

formulation encompasses three different power flow formulations, AC, DC, and interlink converter, and their particular controls for each one.

The paper is organized as follows: Section II describes the primary and secondary controls for both AC and DC microgrids and the interlink converter, considered for the power flow formulation. Section III presents the power flow modelling for the interlink converter, and the AC and DC DG units including primary and secondary controls. Section IV introduces the AC/DC microgrid case study system. Section V outlines the case studies and presents the results obtained. Finally, Section VI provides the conclusions of this work.

II. AC/DC MICROGRID CONTROL

With the purpose to maintain a reliable microgrid operation, different control schemes have to be included for the AC and DC systems, and the interlink converter. These control schemes are presented in detail below.

A. AC microgrid control

The schematic of the two-level hierarchical control incorporated in the AC DG units is shown in Fig. 1; it includes a droop-based primary control, and a secondary control for frequency and voltage restoration [16], [22], [23].

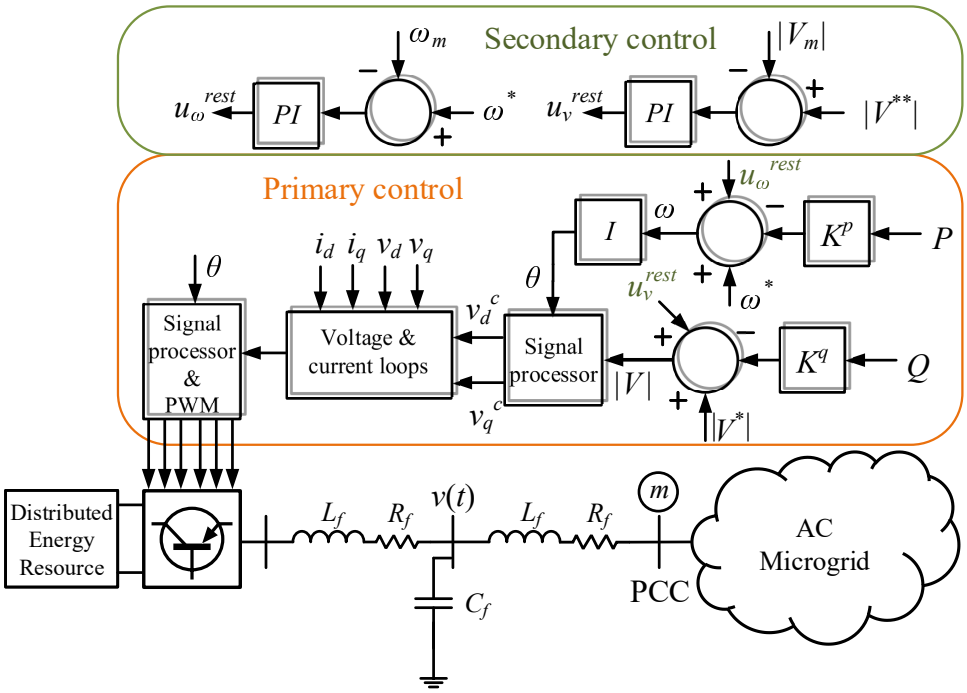

Fig. 1. AC Hierarchical control block diagram.

The primary droop control, including the secondary control, can be expressed by the following set of equations,

$$\omega = \omega^* - K^p P + u_\omega^{rest} \tag{1}$$

$$|V| = |V^*| - K^q Q + u_v^{rest} \tag{2}$$

and

$$u_\omega^{rest} = k^{pw}(\omega^* - \omega_m) + k^{iw} \int (\omega^* - \omega_m) dt \tag{3}$$

$$u_v^{rest} = k^{pv}(|V^{**}| - |V_m|) + k^{iv} \int (|V^{**}| - |V_m|) dt \tag{4}$$

where ω^* is the nominal angular frequency of the system, $|V^*|$ is the voltage amplitude reference, K^p and K^q are the P-ω and Q-V droop coefficients, respectively, P and Q are the output active and reactive power, respectively, ω_m and $|V_m|$ are the angular frequency and the voltage magnitude measured in the bus where the secondary control is connected (m-th bus), respectively, and $|V^{**}|$ is the voltage reference for the secondary control. As is shown in eqs. (1) and (2), the primary control acts as a grid forming scheme, defining the active and reactive power contribution of each DG unit by means of the frequency/active power (P-ω) and voltage/reactive power (Q-V) droop characteristic curves, respectively [22]. On the other hand, the secondary control is responsible for the system frequency and voltage restoration, this is achieved through two proportional-integral (PI) controllers which sends the output signals to each DG unit, as can be seen in Fig. 1 [23].

B. DC microgrid control

The schematic diagram of the two-level hierarchical control incorporated in the DC DG units is shown in Fig.2;

The primary layer includes a (V-P) droop-based dual loop control (inner current and outer voltage loops) [24], [25], while the secondary layer includes a proportional-integral (PI) controller for voltage restoration. Alternatively, primary layer can also be controlled by a using a single (P-V) droop-based current loop. [26]. In both cases, the primary layer control can be expressed using the following equation,

$$V_{DC} = V_{DC}^* - K_{DC}^p P + u_{DC}^{rest} \tag{5}$$

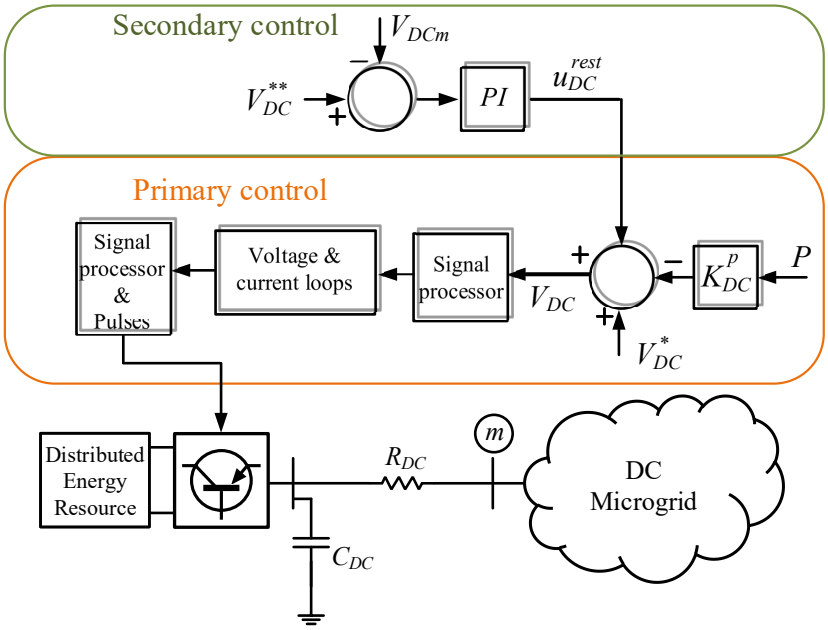

Fig. 2. DC Hierarchical control block diagram.

where V_{DC}^{*} is the voltage reference for the DG converter, K_{DC}^{p} is the droop coefficient corresponding to P-V curve, P is the output power and u_{DC}^{rest} is the restoration voltage obtained from the secondary layer as given by (6) and is also shown in Fig. 2.

$$u_{DC}^{rest} = k_{DC}^{pv}(V_{DC}^{**} - V_{DCm}) + k_{DC}^{iv}\int(V_{DC}^{**} - V_{DCm})dt \tag{6}$$

where V_{DC}^{**} is the voltage reference for the DC microgrid operation, V_{DCm} is the DC voltage where the secondary control is connected (m-th bus), and k_{DC}^{pv} and k_{DC}^{iv} are the proportional and integral gains respectively for the PI controller employed in the secondary control layer. Therefore, the primary layer defines the active power contribution from the DG unit corresponding to the voltage/active power (P-V) droop characteristic curve, while secondary layer is responsible for voltage restoration of the DC microgrid system.

C. Interlink AC/DC converter control

The schematic of the two-level hierarchical control incorporated in the interlink converter is shown in Fig. 3. In order to manage the interlink converter active power, a normalization of the AC system frequency and the DC system voltage magnitude is performed, which allows a proper droop control scheme [15], [27],

$$\hat{\omega} = \frac{\omega - 0.5(\omega_{max} + \omega_{min})}{0.5(\omega_{max} - \omega_{min})} \tag{7}$$

$$\hat{V} = \frac{V_{DC} - 0.5(V_{DCmax} + V_{DCmin})}{0.5(V_{DCmax} - V_{DCmin})} \tag{8}$$

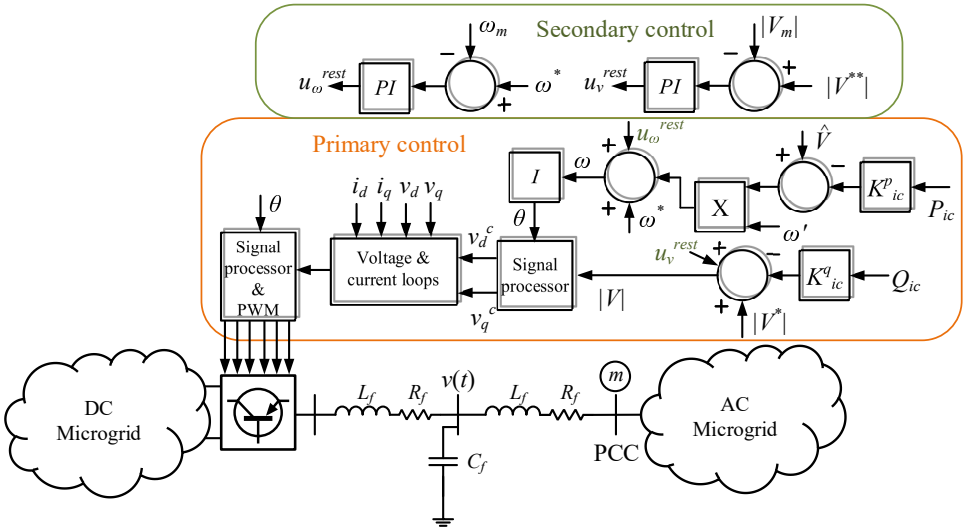

Fig. 3. Interlink converter control block diagram.

Based on the difference between $\hat{\omega}$ and $\hat{V}$, and a droop characteristic gain, the active power droop control scheme for the interlink converter is described as follows,

$$P_{ic} = -\frac{1}{K_{ic}^{p}}(\hat{\omega} - \hat{V}) \tag{9}$$

Note from eq. (9) that, if $\hat{V} > \hat{\omega}$ then P_{ic} is positive, i.e., the interlink converter is injecting active power to the AC system, and if $\hat{V} < \hat{\omega}$ then P_{ic} is negative, i.e., the interlink converter is injecting active power to the DC system. Substituting eq. (7) in (9), the equation can be arranged so that it takes the same form as eq (1), as follows,

$$\omega = \omega^{*} + (\hat{V} - K_{ic}^{p} P_{ic})(\omega') \tag{10}$$

where,

$$\omega' = 0.5(\omega_{max} - \omega_{min}) \tag{11}$$

It can be seen from eq. (10) that active power droop control is included in the primary layer control for the interlink converter, which is very similar to the control scheme shown in Fig. 1. Furthermore, expressing the interlink converter droop control equation in this way allows the inclusion of the secondary frequency control similar to as in the AC DG units droop control as follows,

$$\omega = \omega^* + (\hat{V} - K_{ic}^p P_{ic})(\omega') + u_\omega^{rest} \tag{12}$$

On the other hand, for the reactive power control the same scheme as the one included in the AC DG units is used, therefore, (2) can be used to represent the interlink converter reactive power droop control.

III. Power flow modelling

The principal information obtained from a AC power flow study is the magnitude and the phase angle of the voltage at each system bus, and the real and reactive power flowing through each line [9], from those variables, others can be computed, i.e., line losses, current magnitudes, power factor, etc. One of the most common ways to solve the power flow problem is through the Newton-Raphson method, this method is based in the power flow equations,

$$P_n = \sum_{m=1}^{N} |V_n||V_m||Y_{nm}|cos(\theta_{nm} - \delta_n + \delta_m) \tag{13}$$

$$Q_n = -\sum_{m=1}^{N} |V_n||V_m||Y_{nm}|sin(\theta_{nm} - \delta_n + \delta_m) \tag{14}$$

where n and m represent the different buses of the system, and Y_{nm} is the admittance matrix. These equations constitute a set of nonlinear algebraic equations in terms of the independent variables, voltage magnitude in per unit (p.u.) and phase angle in radians [8]. Expanding (13) and (14) in Taylor's series about the initial estimate and neglecting all higher order terms results in the following set of linear equations [8],

$$\begin{bmatrix} \Delta P_n \\ \Delta Q_n \end{bmatrix} = \begin{bmatrix} \mathbf{J}_1 & \mathbf{J}_2 \\ \mathbf{J}_3 & \mathbf{J}_4 \end{bmatrix} \begin{bmatrix} \Delta\delta_n \\ \Delta|\mathbf{V}_n| \end{bmatrix} \tag{15}$$

where the terms ΔP_n and ΔQ_n are the difference between the scheduled and calculated values. The Jacobian matrix gives the linearized relationship between small changes in voltage angle $\Delta\delta_n$ and voltage magnitude $\Delta|V_n|$ with small changes in real and reactive power ΔP_n and ΔQ_n [8]. Finally, the new estimates for bus voltages are,

$$\delta_n^{(k+1)} = \delta_n^{(k)} + \Delta\delta_n^{(k)} \tag{16}$$

$$|V_n^{(k+1)}| = |V_n^{(k)}| + \Delta|V_n^{(k)}| \tag{17}$$

Using the new voltages, P_n and Q_n are computed again and the process is continued until ΔP_n and ΔQ_n are less than the specified accuracy [8], [9].

For the DC power flow, it is possible to assume the network as pure resistive in its steady state model [13], therefore the power flow equation is,

$$P_{DCn} = \sum_{m=1}^{N} |V_{DCn}||V_{DCm}||Y_{nm}| \tag{18}$$

Using eq. (18), the power flow can be solved as in eq. (15) but only in terms of active power and voltage magnitude. The power flow method is implemented in several professional simulators such as Simulink, Power Factory, among others. However, as mentioned earlier, this conventional method cannot be directly applied to microgrid systems because the DG units power management depends on their control scheme, therefore, different power flow modelling is required depending on the DG units control.

A. AC DG units power flow modelling

From the droop equation (1), it can be seen that the DG unit active power output depends on the frequency of the system, the frequency droop characteristic, and the secondary control output; however, assuming that the secondary control works perfectly, as a result of which the system frequency meets the secondary control frequency reference, i.e., $\omega_m = \omega^*$, the active power equation ends up being as follows,

$$P_n^{ref} = \frac{u_\omega^{rest}}{K_n^p} \tag{19}$$

For the computation of u_ω^{rest}, it has been shown in [17] that the secondary frequency control output depends on the bus angle (δ_m) where the bus is being controlled, and the integration gain (k^{iw}), therefore, the secondary control sets the reference phase angle for all the DG units, making the slack bus unnecessary for the islanded power flow formulation, which in the conventional formulation is required. In this way, the active power equation is as follows [17],

$$P_n^{ref} = \frac{-k^{iw}(\delta_m - \delta_m^0)}{K_n^p} \tag{20}$$

On the other hand, it can be seen from equation (2), that the DG unit reactive power output depends on the voltage magnitude, the voltage droop characteristic, and the secondary voltage output as follows,

$$Q_n^{ref} = \frac{|V_n^*| - |V_n| + u_v^{rest}}{K_n^q} \tag{21}$$

In order to compute u_v^{rest}, it is assume that the secondary voltage control is working perfectly, achieving the voltage reference condition, i.e., $V_m = V^{**}$. Since the voltage of the controlled bus is known (V^{**}),

the reactive equation can be used to numerically compute the value of u_v^{rest} [17]. Note that (20) and (21) constitute the set of equations required to include the hierarchically controlled DG unit model into the conventional power flow in (15). It is worth mentioning that P_n^{ref} and Q_n^{ref} have to be properly escalated to p.u., in order to avoid numerical errors during the solution computation.

B. DC microgrid power flow modelling

The DC power flow modelling only depends on the voltage and active power variables, in this sense, it can be seen from the droop equation (5) that the active power injected from each DG unit depends on the voltage reference, the DC droop characteristic, and the secondary control output,

$$P_{DC}^{ref} = \frac{V_{DCn}^{*} - V_{DCn} + u_{DC}^{rest}}{K_{DCn}^{p}} \tag{22}$$

Note that, as in the reactive power equation from the AC DG unit, in order to compute the secondary signal output u_{DC}^{rest}, it is assumed that the secondary control is working perfectly, achieving $V_{DCm} = V_{DC}^{**}$. Then, the remaining active power equation can be used to numerically compute the secondary control variable. In this way, only eq. (22) is required to include the hierarchically controlled DC DG unit model into the power flow formulation.

C. Interlink AC/DC converter power flow modelling

From the droop equation (12), it can be seen that the interlink converter active power can be expressed as follows,

$$P_{ic}^{ref} = \frac{\omega^{*} - \omega_n + u_{\omega}^{rest}}{\omega' K_{ic}^{p}} + \frac{\hat{V}}{K_{ic}^{p}} \tag{23}$$

Since the secondary frequency control is also included for the interlink converter, the assumption that the system frequency meets the secondary control reference is also valid for this model, furthermore, the computation of u_{ω}^{rest} can be done as shown in eq. (20), therefore, the active power reference equation for the interlink converter power flow formulation is as follows,

$$P_{ic}^{ref} = \frac{-k^{iw}(\delta_m - \delta_m^0)}{\omega' K_{ic}^{p}} + \frac{\hat{V}}{K_{ic}^{p}} \tag{24}$$

Note that the interlink converter active power reference depends on measurements in both AC and DC side, as it was expected from the control scheme.

For the reactive power reference, the same equation from the DG units can be used, this is eq. (21). Note that eqs. (24) and (21), which represent the interlink converter power flow model, set the active

and reactive power for the MG AC side, but the active power has not been set for the MG DC side. For this purpose, the interlink converter is represented in the power flow formulation as two generation buses dependent on each other as shown in Fig 4. Note that the active power reference in the AC side is equal and opposite to that of DC side, i.e., if the interlink converter is injecting active power in the AC microgrid side, it will be absorbing power from the DC microgrid side, and vice versa; in this way, this representation completes the interlink converter model and makes the link between the AC and the DC microgrids. On the other hand, observe in Fig. 4 that, since the LCL capacitor voltage is being controlled by the inverter, the inductor and capacitor are embedded in the power flow formulation, and the capacitor bus is the one considered as the DG unit output.

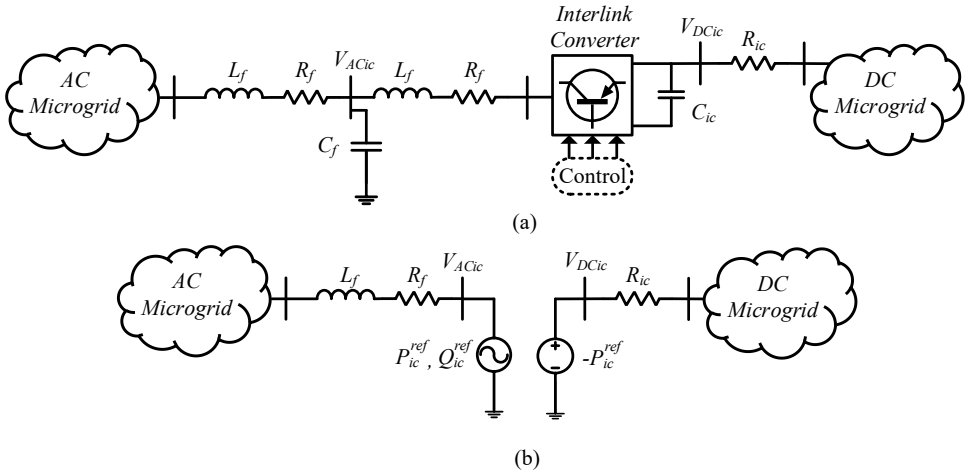

Fig. 4. (a) Single line diagram of the AC/DC hybrid microgrid including the interlink converter; (b) Diagram of the interlink converter power flow model.

It should be noted that, in any of the presented power flow models, the controlled active and reactive power can be restricted due to the power converter capacity, i.e., if the injected power exceeds its specified limit, it is set to the corresponding limit, and the control strategy becomes a constant power control.

IV. Case study system

The case study system is shown in Fig. 5, the AC system includes three hierarchically controlled DG units with an inductive-capacitive-inductive (LCL) filter each one, resistive-inductive (RL) lines between the DG units, and three RL loads. On the other hand the DC system includes two controlled DG units, out of which DG4 includes only primary control and DG5 includes primary and secondary control, which are connected through resistive lines in a ring main circuit, and two resistive loads. The AC DG units and the interlink converter include primary and secondary control, being Bus 5 the one controlled by the secondary control; besides, the DC DG units include primary control, and DG5 includes a secondary

control for controlling the voltage magnitude of Bus 11. Note in Fig. 5, that the LCL filters are marked with a bus label, this is because of the node where the inductances are connected with the capacitor is considered as a system bus. The case study parameters are shown in Table I, note that the same PI control gains are considered for all the DG units; the system parameters and topology were extracted from [17], [24], [25], [28].

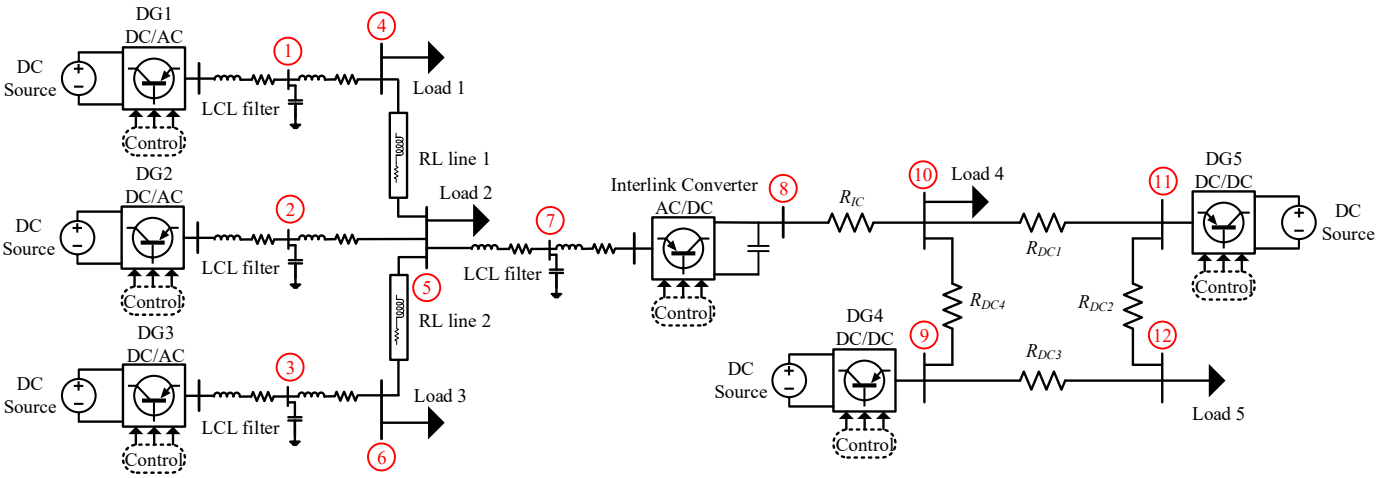

Fig. 5. AC/DC hybrid microgrid single line diagram.

V. Power Flow Model Assessment

In this Section, the evaluation of the proposed hierarchical power flow formulation for AC/DC hybrid microgrids is carried out through two case studies. In the first case, a comparison between the solutions obtained with the power flow formulation and the complete time-domain models using MATLAB/Simulink, is performed. Additionally, the power flow method convergence and the computational (CPU) time required are presented. In this case, the parameters given in Table I are used, note that only linear loads are included, and the DG units have the same droop characteristics for both active and reactive power.

On the other hand, in the second case study the inclusion of voltage dependent industrial loads and different droop characteristics for each DG unit is performed. In this case, similar studies as the ones carried out in the previous case study are presented, showing the proposed method reliability when voltage dependent components are included. The voltage dependent loads are included in Bus 6 and Bus 12, and are expressed as follows [29],

$$P_L = P^0 V^{\alpha} \tag{25}$$

$$Q_L = Q^0 V^{\beta} \tag{26}$$

TABLE I

PARAMETERS OF THE CASE STUDY MICROGRID AND CONTROL

Parameter	Symbol	Value
Nominal AC voltage	V_{L-L}^{RMS}	300 V
Nominal frequency	f*	50 Hz
Base power	S_{base}	100 kVA
Filter resistance	R_f	0.1 Ω
Filter inductance	L_f	1.8 mH
Filter capacitance	C_f	27 μF
Line 1 resistance	R_{Line1}	0.67 Ω
Line 1 inductance	L_{Line1}	1.3 mH
Line 2 resistance	R_{Line2}	0.33 Ω
Line 2 inductance	L_{Line2}	7.96 mH
AC DG units P-ω droop coefficient	K^p	1.25×10^{-5}
AC DG units Q-V droop coefficient	K^q	5×10^{-4}
Interlink P-ω droop coefficient	K_{ic}^p	1.25×10^{-4}
Interlink capacitor	C_{ic}	30×10^{-4} F
AC load resistance	R_{load}	75 Ω
AC load inductance	L_{load}	60 mH
AC active voltage dependent load	P_{AC}^0, α	0.03 p.u., 0.18
AC reactive voltage dependent load	Q_{AC}^0, β	0.015 p.u., 6
Current loop proportional gain	k_{pc}	20
Current loop integral gain	k_{ic}	40
Voltage loop proportional gain	k_{pvo}	2.4×10^{-2}
Voltage loop integral gain	k_{ivo}	4.5
Frec. rest. proportional gain	k^{pw}	0.02
Frec. rest. integral gain	k^{iw}	4
Voltage rest. proportional gain	k^{pv}	0.2
Voltage rest. integral gain	k^{iv}	4
Switching frequency	f_c	10 kHz
Nominal DC voltage	V_{DC}	600 V
DC DG units capacitor	C_{DC}	30×10^{-4} F
DC lines resistance	R_{DC}	0.5 Ω
DC interlink resistance	R_{ic}	0.3 Ω
DC load resistance	R_{DCload}	180 Ω
DC voltage dependent load	P_{DC}^0, α	0.02 p.u., 0.18
DC DG units P-V droop coefficient	K_{DC}^p	0.5
DC Current loop proportional gain	k_{DC}^{pc}	0.33
DC Current loop integral gain	k_{DC}^{ic}	15
DC Voltage loop proportional gain	k_{DC}^{pvo}	1.75
DC Voltage loop integral gain	k_{DC}^{ivo}	10
DC Voltage rest. proportional gain	k_{DC}^{pv}	1.75
DC Voltage rest. integral gain	k_{DC}^{iv}	100

where $\alpha = 0.18$, $\beta = 6$, $P^0_{AC} = 0.03$ p.u., $Q^0_{AC} = 0.015$ p.u., $P^0_{DC} = 0.02$ p.u., and $S_{base} = 100$ kVA. The droop characteristics of each DG unit are shown in Table II. It should be highlighted that the proposed power flow model does not include the harmonics due to distorting loads and other harmonic sources, but is suitable for voltage dependent loads that do not inject harmonics in the system. For conventional power systems, generally harmonics can be included in the power flow formulation using current source injection methods [30], however, for microgrids with hierarchical control, dynamics of primary and secondary layers along with their interaction with converter dynamics need to be considered for harmonic power flow formulation.

The studies were performed in a Lenovo ThinkPad with a processor of 1.6 GHz Intel Core i5-8250U and 8 GB of RAM. A convergence error tolerance of 1×10^{-8} was used.

TABLE II

DROOP CHARACTERISTIC PARAMETERS FOR CASE STUDY II

Parameter	Symbol	Value
AC DG 1 P-ω droop coefficient	K^p_1	2.5×10^{-5}
AC DG 1 Q-V droop coefficient	K^q_1	6.0×10^{-4}
AC DG 2 P-ω droop coefficient	K^p_2	1.3×10^{-5}
AC DG 2 Q-V droop coefficient	K^q_2	3.0×10^{-4}
AC DG 3 P-ω droop coefficient	K^p_3	4.3×10^{-5}
AC DG 3 Q-V droop coefficient	K^q_3	4.0×10^{-4}
DC DG 4 P-V droop coefficient	K^p_{DC4}	0.3
DC DG 5 P-V droop coefficient	K^p_{DC5}	0.5

A. Case study I: AC/DC hybrid microgrid power flow evaluation

Table III shows the steady-state voltage magnitudes, phase angle, active power, and reactive power obtained with the proposed power flow formulation, and MATLAB/Simulink. It may be noted in Table III that, each bus is explicitly defined as either AC PQ, DC P, AC DG, AC IC, and DC IC, so that buses with DG units can be highlighted. Additionally, it is worthwhile observe that the load buses (PQ buses) do not have any active and reactive power output, this is because in order to take into account the effect of the bus voltage in the RL loads, the loads are included in the admittance matrix ($\mathbf{Y}$), then, the PQ buses in the power flow formulation have $P^{ref} = 0$ and $Q^{ref} = 0$.

Since the MATLAB/Simulink system takes into account only fundamental frequency, i.e., the DG unit converters are modeled as average models, it is expected that, if the proposed power flow models are correct, the steady-state results from the simulator match almost equally with the power flow results, just having integration errors due to the integration method and time-step from the simulator. In this way, it

TABLE III

CASE STUDY I: RESULTS COMPARISON BETWEEN THE PROPOSED HIERARCHICAL POWER FLOW METHOD AND MATLAB/SIMULINK

		Proposed Power Flow				MATLAB/Simulink (25 s simulated)			
Bus	Bus type	Voltage (p.u.)	Angle (rad)	Active Power (W)	Reactive Power (VAr)	Voltage (p.u.)	Angle (rad)	Active Power (W)	Reactive Power (VAr)
1	AC DG	1.00229	1.57641	1254.25	124.68	1.00229	1.57641	1254.36	124.63
2	AC DG	1.00226	1.57458	1254.25	143.61	1.00226	1.57458	1254.36	143.62
3	AC DG	1.00208	1.57813	1254.25	247.42	1.00208	1.57813	1254.36	247.41
4	AC PQ	1.00015	1.56869	-	-	1.00015	1.56869	-	-
5	AC PQ	1.00000	1.56687	-	-	1.00000	1.56687	-	-
6	AC PQ	0.99917	1.57053	-	-	0.99917	1.57053	-	-
7	AC IC	1.00188	1.56413	-372.15	367.46	1.00188	1.56412	-372.46	367.9
8	DC IC	0.99855	-	372.15	-	0.99855	-	372.46	-
9	DC DG	0.99874	-	903.73	-	0.99874	-	904.01	-
10	DC P	0.99824	-	-	-	0.99824	-	-	-
11	DC DG	1.00000	-	2714.75	-	1.00000	-	2715.3	-
12	DC P	0.99798	-	-	-	0.99798	-	-	-

can be seen in Table III that the steady-state voltage magnitude and phase angle from the proposed power flow match with the MATLAB/Simulink results; however, the active and reactive power results have small differences between the power flow and the simulator, which are associated with the simulator integration method, time-step, and measurement blocks. In this way, the obtained results confirm the reliability of the proposed hierarchical power flow models for AC/DC hybrid microgrids.

TABLE IV

CONVERGENCE ERRORS OF THE CASE I

Iteration	Proposed Power Flow
1	0.0014
2	6.5688×10^{-6}
3	6.8823×10^{-11}
CPU time	0.1017 s

Generally the important and desired features for any power flow studies are computational speed and convergence rate, in this regard, Table IV shows the iterations and CPU time required to solve the power flow problem. Note that, the Newton-Raphson method, which is used to solve the power flow equations, offers quadratic convergence rate, requiring only three iterations to get an error of 6.8823×10^{-11} with a CPU time of 0.1017 seconds, therefore, showing the effectiveness and advantages of using the proposed power flow models even when AC/DC hybrid microgrids are assessed.

TABLE V

CASE STUDY II: RESULTS COMPARISON BETWEEN THE PROPOSED HIERARCHICAL POWER FLOW METHOD AND MATLAB/SIMULINK

		Proposed Power Flow				MATLAB/Simulink (25 s simulated)			
Bus	Bus type	Voltage (p.u.)	Angle (rad)	Active Power (W)	Reactive Power (VAr)	Voltage (p.u.)	Angle (rad)	Active Power (W)	Reactive Power (VAr)
1	AC DG	1.00411	1.57491	1604.32	26.55	1.00411	1.57491	1604.39	26.52
2	AC DG	1.00403	1.57993	3085.23	129.12	1.00403	1.57993	3085.38	129.13
3	AC DG	1.00218	1.50693	932.74	1488.32	1.00218	1.50693	932.79	1488.33
4	AC PQ	1.00222	1.56492	-	-	1.00222	1.56492	-	-
5	AC PQ	1.00000	1.56076	-	-	1.00000	1.56076	-	-
6	AC PQ	0.99182	1.50269	-2995.57	-1427.93	0.99182	1.50270	-2995.65	-1427.95
7	AC IC	1.00321	1.55807	-328.96	571.99	1.00321	1.55807	-329.20	571.58
8	DC IC	0.99863	-	328.96	-	0.99863	-	329.20	-
9	DC DG	0.99904	-	1145.82	-	0.99904	-	1146.15	-
10	DC P	0.99836	-	-	-	0.99836	-	-	-
11	DC DG	1.00000	-	2523.32	-	1.00000	-	2523.65	-
12	DC P	0.99813	-	-1999.18	-	0.99813	-	-1998.85	-

B. Case study II: AC/DC hybrid microgrid power flow evaluation including voltage dependent components

The steady-state voltage magnitudes, phase angles, and active and reactive powers obtained with the proposed power flow formulation and MATLAB/Simulink are shown in Table V. Note that, even with including voltage dependent loads and different droop characteristics for each DG unit, the results with the power flow match with the ones obtained with MATLAB/Simulink, having negligibly small differences among the active and reactive powers between the two approaches, which are associated with the simulator solver.

TABLE VI

CONVERGENCE ERRORS OF THE CASE II

Iteration	Proposed Power Flow
1	0.0130
2	1.3846×10^{-4}
3	5.7861×10^{-8}
4	1.9679×10^{-14}
CPU time	0.1545 s

On the other hand, Table VI shows the Newton-Raphson method performance details; observe that in this case, due to the voltage dependent loads, the method requires 4 iterations to compute the steady-state solution, achieving a convergence error of 1.9679×10^{-14} and requiring 0.1545 seconds. Even though in

this case the CPU time is increased, it is still a fast tool for steady-state analyzes. Moreover, the results obtained shown the power flow formulation reliability and efficiency even working with voltage dependent scenarios.

VI. Conclusion

This paper has introduced a comprehensive power flow modeling for the hierarchically controlled hybrid AC/DC microgrids. The proposed model includes the effects of primary and secondary control layers in the conventional Newton-Raphson-based power flow formulation, thereby makes it suitable for the hybrid AC/DC microgrid applications with power electronically controlled intermittent DG units. The proposed model not only includes AC and DC microgrid control characteristics but also presents the detailed power flow modeling for the interlink converter responsible for power exchange between AC and DC microgrid units. The efficacy and accuracy of the proposed model are validated by comparing its results with results obtained through a professional simulator i.e. MATLAB/SIMULINK. The results showed that the proposed scheme is capable of accurately modeling power flow for a hybrid AC/DC microgrid working under linear and voltage dependent loading conditions. Moreover, it has also been demonstrated that the power flow achieves fast CPU times with quadratic convergence, such that the solutions can be obtained within three iterations for the linear loading scenario and within four iterations for the voltage dependent loading scenario. Therefore, the proposed power flow model can be regarded as an efficient as well as a reliable tool for future power flow planning and operation studies in hybrid AC/DC microgrid environments.

Acknowledgement

This work was funded by a Villum Investigator grant (no. 25920) from The Villum Fonden.

References

[1] E. Aprilia, K. Meng, M. Al Hosani, H. H. Zeineldin, and Z. Y. Dong, "Unified power flow algorithm for standalone ac/dc hybrid microgrids," *IEEE Transactions on Smart Grid*, vol. 10, no. 1, pp. 639–649, Jan 2019.

[2] H. M. A. Ahmed, A. B. Eltantawy, and M. M. A. Salama, "A generalized approach to the load flow analysis of ac–dc hybrid distribution systems," *IEEE Transactions on Power Systems*, vol. 33, no. 2, pp. 2117–2127, March 2018.

[3] M. Nasir and H. A. Khan, "Solar photovoltaic integrated building scale hybrid ac/dc microgrid," in *5th IET International Conference on Renewable Power Generation, London, United Kingdom*. IET, 2016.

[4] Y. Xia, Y. Peng, P. Yang, M. Yu, and W. Wei, "Distributed coordination control for multiple bidirectional power converters in a hybrid ac/dc microgrid," *IEEE Transactions on Power Electronics*, vol. 32, no. 6, pp. 4949–4959, June 2017.

[5] C. Li, S. K. Chaudhary, M. Savaghebi, J. C. Vasquez, and J. M. Guerrero, "Power flow analysis for low-voltage ac and dc microgrids considering droop control and virtual impedance," *IEEE Transactions on Smart Grid*, vol. 8, no. 6, pp. 2754–2764, Nov 2017.

[6] J. Schiffer, D. Zonetti, R. Ortega, A. Stankovic, T. Sezi, and J. Raisch, "A survey on modeling of microgrids - from fundamental physics to phasors and voltage sources," *ArXiv*, May 2015.

[7] S. Chowdhury and P. Crossley, *Microgrids and Active Distribution Networks*, ser. IET renewable energy series. Institution of Engineering and Technology, 2009.

[8] H. Saadat, *Power System Analysis*, ser. McGraw-Hill series in electrical and computer engineering. McGraw-Hill, 2002.

[9] W. Stevenson and J. Grainger, *Power System Analysis*, ser. McGraw-Hill series in electrical and computer engineering: Power and energy. McGraw-Hill Education (India) Pvt Limited, 2003.

[10] M. Nasir, S. Iqbal, and H. A. Khan, "Optimal planning and design of low-voltage low-power solar dc microgrids," *IEEE Transactions on Power Systems*, vol. 33, no. 3, pp. 2919–2928, 2017.

[11] M. M. A. Abdelaziz, H. E. Farag, E. F. El-Saadany, and Y. A. R. I. Mohamed, "A novel and generalized three-phase power flow algorithm for islanded microgrids using a newton trust region method," *IEEE Transactions on Power Systems*, vol. 28, no. 1, pp. 190–201, Feb 2013.

[12] M. H. Moradi, V. B. Foroutan, and M. Abedini, "Power flow analysis in islanded micro-grids via modeling different operational modes of dgs: A review and a new approach," *Renewable and Sustainable Energy Reviews*, vol. 69, no. Supplement C, pp. 248 – 262, 2017.

[13] C. Li, S. K. Chaudhary, J. C. Vasquez, and J. M. Guerrero, "Power flow analysis for droop controlled lv hybrid ac-dc microgrids with virtual impedance," in *2014 IEEE PES General Meeting — Conference Exposition*, July 2014, pp. 1–4.

[14] A. A. Hamad, M. A. Azzouz, and E. F. El Saadany, "A sequential power flow algorithm for islanded hybrid ac/dc microgrids," *IEEE Transactions on Power Systems*, vol. 31, no. 5, pp. 3961–3970, Sep. 2016.

[15] A. A. Eajal, M. A. Abdelwahed, E. F. El-Saadany, and K. Ponnambalam, "A unified approach to the power flow analysis of ac/dc hybrid microgrids," *IEEE Transactions on Sustainable Energy*, vol. 7, no. 3, pp. 1145–1158, July 2016.

[16] J. M. Guerrero, J. C. Vasquez, J. Matas, L. G. de Vicuna, and M. Castilla, "Hierarchical control of droop-controlled ac and dc microgrids: A general approach toward standardization," *IEEE Transactions on Industrial Electronics*, vol. 58, no. 1, pp. 158–172, Jan 2011.

[17] G. Agundis-Tinajero, J. Segundo-Ramírez, N. Visairo-Cruz, M. Savaghebi, J. M. Guerrero, and E. Barocio, "Power flow modeling of islanded ac microgrids with hierarchical control," *International Journal of Electrical Power Energy Systems*, vol. 105, pp. 28 – 36, 2019.

[18] Y. Xia, W. Wei, M. Yu, Y. Peng, and J. Tang, "Decentralized multi-time scale power control for a hybrid ac/dc microgrid with multiple subgrids," *IEEE Transactions on Power Electronics*, vol. 33, no. 5, pp. 4061–4072, May 2018.

[19] D. E. Olivares, A. Mehrizi-Sani, A. H. Etemadi, C. A. Cañizares, R. Iravani, M. Kazerani, A. H. Hajimiragha, O. Gomis-Bellmunt, M. Saeedifard, R. Palma-Behnke, G. A. Jiménez-Estévez, and N. D. Hatziargyriou, "Trends in microgrid control," *IEEE Transactions on Smart Grid*, vol. 5, no. 4, pp. 1905–1919, July 2014.

[20] Y. Xia, W. Wei, M. Yu, X. Wang, and Y. Peng, "Power management for a hybrid ac/dc microgrid with multiple subgrids," *IEEE Transactions on Power Electronics*, vol. 33, no. 4, pp. 3520–3533, April 2018.

[21] P. Yang, M. Yu, Q. Wu, N. Hatziargyriou, Y. Xia, and W. Wei, "Decentralized bidirectional voltage supporting control for multi-mode hybrid ac/dc microgrid," *IEEE Transactions on Smart Grid*, pp. 1–1, 2019.

[22] J. M. Guerrero, L. G. de Vicuna, J. Matas, M. Castilla, and J. Miret, "A wireless controller to enhance dynamic performance of parallel inverters in distributed generation systems," *IEEE Transactions on Power Electronics*, vol. 19, no. 5, pp. 1205–1213, Sept 2004.

[23] J. Rocabert, A. Luna, F. Blaabjerg, and P. Rodríguez, "Control of power converters in ac microgrids," *IEEE Transactions on Power Electronics*, vol. 27, no. 11, pp. 4734–4749, Nov 2012.

[24] M. Nasir, M. Anees, H. A. Khan, and J. M. Guerrero, "Dual-loop control strategy applied to the cluster of multiple nanogrids for rural electrification applications," *Iet Smart Grid*, vol. 2, no. 3, pp. 327–335, 2019.

[25] M. Nasir, H. A. Khan, K. A. K. Niazi, Z. Jin, and J. M. Guerrero, "Dual-loop control strategy applied to pv/battery-based islanded dc microgrids for swarm electrification of developing regions," *The Journal of Engineering*, vol. 2019, no. 18, pp. 5298–5302, 2019.

[26] C. Jin, P. Wang, J. Xiao, Y. Tang, and F. H. Choo, "Implementation of hierarchical control in dc microgrids," *IEEE transactions on industrial electronics*, vol. 61, no. 8, pp. 4032–4042, 2013.

[27] P. C. Loh, D. Li, Y. K. Chai, and F. Blaabjerg, "Autonomous operation of hybrid microgrid with ac and dc subgrids," *IEEE Transactions on Power Electronics*, vol. 28, no. 5, pp. 2214–2223, May 2013.

[28] F. Katiraei and M. Iravani, "Power management strategies for a microgrid with multiple distributed generation units," *IEEE Transactions on Power Systems*, vol. 21, no. 4, pp. 1821–1831, Nov 2006.

[29] A. M. Vural, "Interior point-based slack-bus free-power flow solution for balanced islanded microgrids," *International Transactions on Electrical Energy Systems*, vol. 26, no. 5, pp. 968–992, 2016.

[30] D. Xia and G. T. Heydt, "Harmonic power flow studies part i - formulation and solution," *IEEE Transactions on Power Apparatus and Systems*, vol. PAS-101, no. 6, pp. 1257–1265, 1982.